

The Synthesis and Spectroscopic Properties of Macrocyclic Polyethers Containing Two Different Aromatic Moieties and Their [2]Catenanes Incorporating Cyclobis(paraquat-*p*-phenylene)**

Roberto Ballardini,* Vincenzo Balzani,* Maria Teresa Gandolfi, Richard E. Gillard, J. Fraser Stoddart,* and Elena Tabellini

Abstract: The synthesis of six derivatives of bis-*p*-phenylene-34-crown-10 (BPP34C10) in which one or both of the *p*-phenylene rings are replaced by other π -electron-rich aromatic ring systems, and their subsequent use as templates for the self-assembly of the tetracationic cyclophane cyclobis(paraquat-*p*-phenylene) and thus the construction of [2]catenanes, are described. The *p*-phenylene rings in BPP34C10 have been replaced variously by *p*-xylyl units, 1,5-, 1,6-, 2,6- and 2,7-naphtho units, and a naphthalene-2,6-dimethyl ring system in the six new crown ether derivatives. Five of the [2]catenanes have the potential to exist in solution as equilibrating mixtures of two translational isomers, the proportions of which have been determined in solution by dynamic ¹H NMR spectroscopy. The absorption

spectra and luminescence properties (fluorescence, phosphorescence, and excitation spectra, excitation state lifetimes, and fluorescence quantum yields) of the BPP34C10 derivatives (in which one of the *p*-phenylene rings has been replaced by either a *p*-xylyl unit or a naphthalene-2,6-dimethyl unit or where both of the *p*-phenylene rings have been replaced, one by a *p*-xylyl unit and the other by a 1,5-naphtho unit) and their derived [2]catenanes, with cyclobis(paraquat-*p*-phenylene) as the interlocking cyclophane component, have been investigated. Comparison with the properties of simple model compounds

shows the presence of intra- and intermolecular electronic interactions between the component units of the crown ethers and catenanes. The main consequences of these interactions in the crown ethers are small perturbations in the absorption spectra of the two chromophoric units, and strong changes in the luminescence properties due to the occurrence of intercomponent energy-transfer processes and charge-transfer (CT) interactions. In the [2]catenanes, perturbations in the absorption spectra of the component units of the crown ether and tetracationic cyclophane, accompanied by the appearance of CT absorption bands in the visible region, and complete luminescence quenching caused by the presence of low-energy CT levels are observed.

Keywords: catenanes • charge transfer • luminescence • self-assembly • translational isomerism

Introduction

Self-assembly processes,^[1] which are widespread in biological systems, are currently being employed by synthetic chemists for the construction of nanometer-scale compounds and complexes.^[2] Conventional organic synthesis can be used to synthesize subunits that can recognize^[3] one another through noncovalent bonding interactions to afford stable, well-defined molecular assemblies and supramolecular^[4] arrays.

The interactions between π -electron acceptors (e.g., the paraquat dication^[5]) and π -electron donors (e.g., the hydroquinone unit^[6]) have provided the inspiration for the synthesis of a wide range of mechanically interlocked structures.^[7] It may be recalled that the [2]catenane **4**⁴⁺, comprised of bis-*p*-phenylene-34-crown-10 (BPP34C10) and cyclobis(paraquat-*p*-phenylene), is formed in a remarkable 70% yield^[8] at ambient pressure in MeCN (Scheme 1), where **3** acts as a template for the reaction of **2** with **1**⁴⁺. The efficiency of this catenation is, in part, a result of the high level of preorganiza-

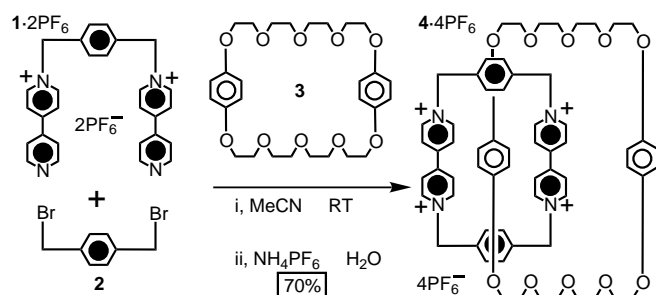
[*] Prof. J. F. Stoddart,^[+] Dr. R. E. Gillard
School of Chemistry, University of Birmingham
Edgbaston, Birmingham B15 2TT (UK)

Dr. R. Ballardini
Istituto FRAE-CNR, via Gobetti 101
I-40129 Bologna (Italy)
Fax: (+39)51-6399-844

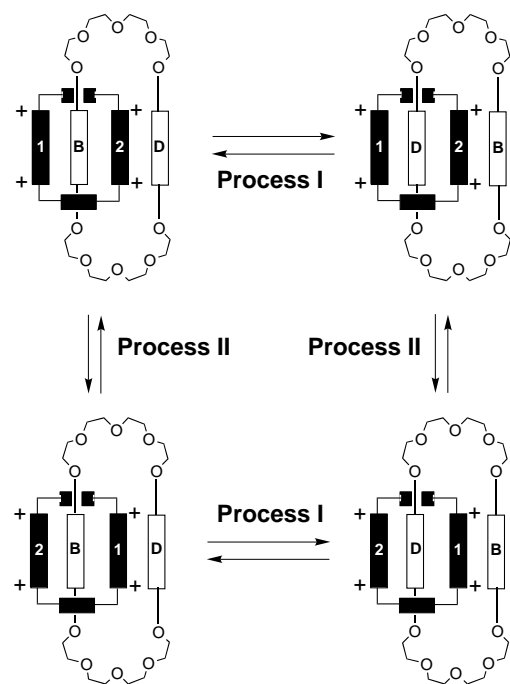
Prof. V. Balzani, Prof. M. T. Gandolfi, Dr. E. Tabellini
Dipartimento di Chimica G. Ciamician, Università di Bologna
Via Selmi 2, I-40126 Bologna (Italy)
Fax: (+39)51-259456

[+] Current address
Department of Chemistry and Biochemistry
University of California at Los Angeles
405 Hilgard Avenue, Los Angeles, CA90095 (USA)
Fax: (+1)310-206-1843
E-mail: stoddart@chem.ucla.edu

[**] Molecular Meccano, Part 31. For Part 30, see D. B. Amabilino, P. R. Ashton, V. Balzani, S. E. Boyd, A. Credi, J. Y. Lee, S. Menzer, J. F. Stoddart, M. Venturi, D. J. Williams, *J. Am. Chem. Soc.*, submitted.

Scheme 1. The self-assembly of the [2]catenane $4 \cdot 4\text{PF}_6$.

tion present in the macrocyclic polyether. The [2]catenane is stabilized by π - π stacking,^[9] as well as by [C-H...O] hydrogen bonding^[10] and T-type^[11] interactions. Dynamic ^1H NMR spectroscopy reveals that the [2]catenane is, not surprisingly, highly ordered in solution. At 25 °C each of the macrocyclic rings is circumrotating through the cavity of the other macrocyclic ring. The two dynamic processes are distinct and observable by ^1H NMR spectroscopy (Scheme 2).^[12] [2]Catenanes in which one of the ring components incorporates two different aromatic units can potentially exist as two translational isomers.^[13] In principle, control over the thermodynamic equilibrium associated with translational isomerism can be achieved by either steric or electronic means.

Scheme 2. The two dynamic processes (I and II) that are distinct and observable by ^1H NMR spectroscopy.

Considerable effort has been devoted to changing the nature of the π -electron acceptor and donor units in the ring components of the [2]catenane 4^{4+} . The bipyridinium units of the tetracationic cyclophane have been replaced by *trans*-1,2-bis(pyridinium)ethylene^[14] and 2,7-diazapyrenium units.^[15]

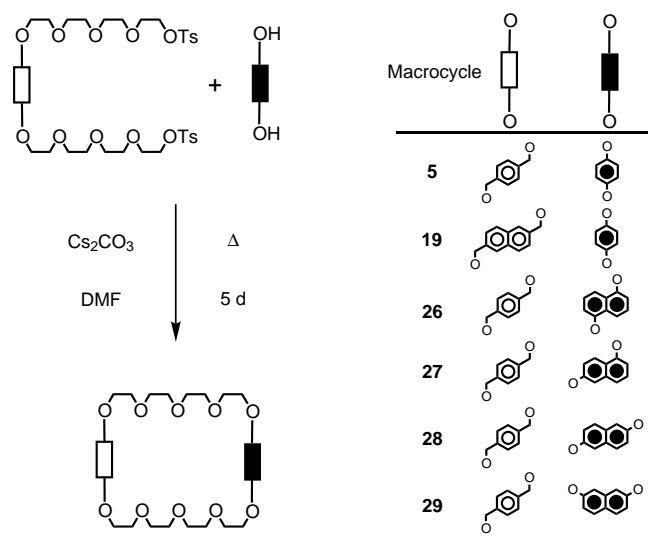
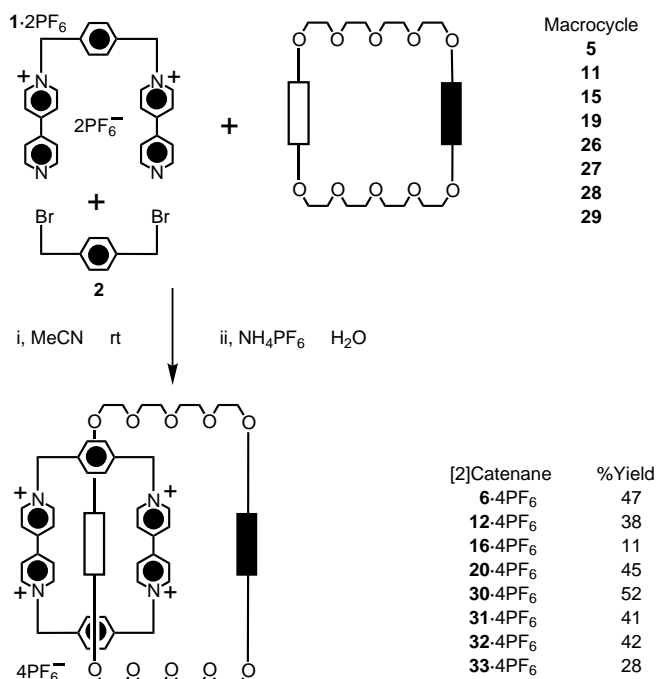
This paper records results that relate to changing the nature of the neutral macrocyclic polyether component of the [2]catenane. Translational isomerism in [2]catenanes that incorporate two different aromatic π -electron-rich units in the macrocyclic polyether component is determined by the balance between π - π stacking interactions and solvation. Here, the incorporation of *p*-xylyl units and 1,5-, 1,6-, 2,6-, and 2,7-naphtho ring systems into the macrocyclic polyether component will be discussed.

Electronic interactions between subunits play an important role in determining the structure and reactivity of multi-component species.^[4, 16] For the design of more efficient chemical,^[17] photochemical,^[18] and electrochemical^[17a, 18d, 19] molecular devices based on rotaxanes and catenanes it is necessary to investigate the behavior of these interlocked molecules containing the new components and to extend our knowledge of the intercomponent interactions. Each one of the crown ethers **5**, **19**, and **26** illustrated in Scheme 3 contains two distinct chromophoric and luminescent units. It is interesting to compare their absorption and luminescence properties with those of simple model compounds in order to elucidate the degree of intercomponent interaction and the occurrence of energy-transfer processes. In the [2]catenanes 6^{4+} , 20^{4+} , and 30^{4+} illustrated in Scheme 4, the electron-donor units of the crown ethers are expected to undergo charge-transfer (CT) interactions with the electron-acceptor bipyridinium units of the tetracationic cyclophane with profound changes in the absorption and luminescence properties.

Results and Discussion

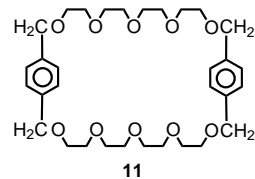
Incorporation of *p*-xylyl units into the macrocyclic polyether component: The hydroquinone rings contained in macrocyclic polyethers are π -electron rich. It seemed logical, therefore, that replacing the phenolic oxygen atoms with benzylic methylene groups would decrease the π -electron-donating nature of the *p*-phenylene ring(s) in the macrocyclic polyether component. *p*-Phenylene-*p*-xylyl-36-crown-10 (**5**) has been synthesized (Scheme 3) in 23% yield. The catenation of **5** with cyclobis(paraquat-*p*-phenylene) gave the [2]catenane $6 \cdot 4\text{PF}_6$ in 47% yield (Scheme 4). In CD_3COCD_3 solution at 233 K, the ratio of translational isomers was 88:12 in favor of the hydroquinone ring residing inside the tetracationic cyclophane. In the more polar solvent CD_3CN at the same temperature, this ratio decreased to 61:39.

Clearly, the tetracationic cyclophane is able to accept the *p*-xylyl unit into its cavity. In fact, the acyclic polyether *α,α'*-bis[2-(2-hydroxyethoxy)ethoxy]-*p*-xylene (**7**) is bound by cyclobis(paraquat-*p*-phenylene) ($8 \cdot 4\text{PF}_6$) with an association constant of 1900M^{-1} (cf. 2200M^{-1} for the binding of the acyclic polyether 1,4-bis[2-(2-hydroxyethoxy)ethoxy]benzene (**9**) with $8 \cdot 4\text{PF}_6$).^[20] The propensity of the *p*-xylyl unit to be included inside the cavity of the tetracationic cyclophane $8 \cdot 4\text{PF}_6$ is probably a consequence of the electrostatic interactions between the oxygen atoms adjacent to the *p*-xylyl unit and the dicationic bipyridinium units of the tetracationic cyclophane, as well as of π - π stacking. Thus, it should be

Scheme 3. Synthesis of the macrocyclic polyethers **5**, **19**, and **26–29**.Scheme 4. The self-assembly of the [2]catenanes, **6**·4PF₆, **12**·4PF₆, **16**·4PF₆, **20**·4PF₆, and **30**·4PF₆–**33**·4PF₆. Note that the constitutions of these [2]catenanes can be deduced from the key in Scheme 3.

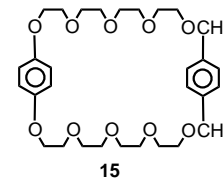
possible to assemble a [2]catenane that incorporates a macrocyclic polyether containing two *p*-xylyl units and **8**·4PF₆.

Bis-*p*-xylyl-38-crown-10 (**11**) was synthesized by the reaction of tetraethylene glycol (**10**) with 1,4-bis(bromomethyl)benzene (**2**) in the presence of NaH under high dilution conditions. The catenation of **11** with **8**·4PF₆ gave the [2]catenane **12**·4PF₆ in 38% yield (Scheme 4). At 333 K in CD₃CN, ¹H NMR spectroscopy of **12**·4PF₆ showed a signal at $\delta = 5.12$ for eight



aromatic protons that corresponds to the averaged resonance for the inside and alongside *p*-xylyl units, indicating that Process I (Scheme 2) is fast on the ¹H NMR timescale. On cooling a CD₃COCD₃ solution of the [2]catenane down to 233 K, two signals can be observed corresponding to aromatic protons on the *p*-xylyl units located inside ($\delta = 4.02$) and alongside ($\delta = 7.00$) the cavity of the tetracationic cyclophane. The energy barrier associated with this process was calculated from the line broadening^[21] of the signal at $\delta = 7.00$ to be 11.9 kcal mol⁻¹, that is, 3.7 kcal mol⁻¹ less than for the same process in the [2]catenane **4**·4PF₆. This decrease in the energy barrier for Process I is a consequence of the weaker interactions between the macrocyclic polyether component and the tetracationic cyclophane in **12**·4PF₆ compared with **4**·4PF₆.

Since the *p*-xylyl unit of the macrocyclic polyethers **5** and **11** has the propensity to be included inside the cavity of the tetracationic cyclophane, it was decided to remove the oxygen atoms adjacent to the *p*-xylyl unit completely in order to influence further the ratio of the translational isomers. To this end, the 34-crown-8 derivative **15** was synthesized in 34% yield from 1,4-bis[2-[2-(2-*p*-toluenesulfonylethoxy)ethoxy]benzene (**13**) and 1,4-phenylene dipropanol (**14**) in the presence of NaH under high dilution conditions. The catenation of **15** with **8**·4PF₆ gave the [2]catenane **16**·4PF₆ in 11% yield (Scheme 3).



In both CD₃COCD₃ and CD₃CN solutions over the range of accessible temperatures, only one translational isomer could be observed for **16**·4PF₆ by ¹H NMR spectroscopy, that is, the one with the hydroquinone ring located inside ($\delta = 3.90$, CD₃COCD₃) and the *p*-xylyl unit located alongside ($\delta = 6.59$, CD₃COCD₃) the tetracationic cyclophane. Process I could not be observed for this [2]catenane although we anticipate that circumrotation does occur. However, the coalescence of two signals corresponding to the α -CH protons of the bipyridinium units located inside and alongside the cavity of the macrocyclic polyether at 205 K is consistent with Process II (Scheme 2) becoming fast on the ¹H NMR timescale. The energy barrier for this process was calculated, by means of the coalescence approach,^[22] to be 9.2 kcal mol⁻¹, that is, 3.0 kcal mol⁻¹ lower than the same process in the [2]catenane **4**·4PF₆. The lower energy barrier for this process, compared with that for **4**·4PF₆, is almost certainly a consequence of the poor recognition displayed between the *p*-xylyl unit and the tetracationic cyclophane in the [2]catenane **16**·4PF₆; an observation supported by the decrease in the efficiency of the self-assembly process (11% yield of **16**·4PF₆ compared with 70% yield for **4**·4PF₆).

Incorporation of naphthalene-2,6-dimethyl in the macrocyclic polyether component: The macrocyclic polyether naphthalene-2,6-dimethyl-*p*-phenylene-38-crown-10 (**19**) was synthesized from **17** and hydroquinone (**18**) in 18% yield (Scheme 3). The catenation of **19** with **8**·4PF₆ gave the [2]catenane **20**·4PF₆ in 45% yield (Scheme 4). Dynamic ¹H NMR spectroscopy of this [2]catenane in CD₃COCD₃ solu-

tion revealed the presence of only one translational isomer—that with the hydroquinone ring located inside the cavity of the tetracationic cyclophane. In CD_3CN solution, a small amount (5%) of the other translational isomer could be observed. These observations are in accordance with the low binding constant ($K_a = 796\text{M}^{-1}$ in MeCN at 298 K) of the acyclic naphthalene-2,6-dimethyl-yl-containing polyether, compared with that of the hydroquinone-containing polyether.

Incorporation of *p*-xylyl and dioxynaphthalene units in the macrocyclic polyether component: A series of macrocyclic polyethers, incorporating dioxynaphthalene units with different substitution patterns and a *p*-xylyl unit, have been synthesized. The bistosylate **21** was reacted with either 1,5-, 1,6-, 2,6-, or 2,7-dihydroxynaphthalene (**22**, **23**, **24**, and **25**, respectively) in the presence of Cs_2CO_3 under high dilution conditions to give the macrocyclic polyethers in yields of 12 to 53% (Scheme 3). The catenations of the macrocyclic polyethers **26**, **27**, **28**, and **29** with $8 \cdot 4\text{PF}_6$ gave the [2]catenanes $30 \cdot 4\text{PF}_6$, $31 \cdot 4\text{PF}_6$, $32 \cdot 4\text{PF}_6$, and $33 \cdot 4\text{PF}_6$ in 52, 41, 42, and 28% yields, respectively (Scheme 4).

Dynamic ^1H NMR spectroscopy revealed both solvent and temperature dependences upon the equilibrium position of the translational isomerism in [2]catenane $30 \cdot 4\text{PF}_6$. In CD_3COCD_3 , and also in CD_3CN solution, the 1,5-dioxynaphthalene unit resides preferentially inside the cavity of the tetracationic cyclophane. In CD_3COCD_3 , the ratio is 60:40 at 282 K, increasing to 81:19 on cooling to 193 K. In CD_3CN , the ratio is 54:46 at 281 K, increasing to 73:27 on cooling to 228 K.

In the case of the [2]catenanes $31 \cdot 4\text{PF}_6$ – $33 \cdot 4\text{PF}_6$, in CD_3COCD_3 and CD_3CN , only one translational isomer can be observed—that in which the *p*-xylyl unit is located inside the cavity of the tetracationic cyclophane. This result is presumably a consequence of the better steric match between the *p*-xylyl unit and the bipyridinium units of the tetracationic cyclophane when compared with that between the 1,6-, 2,6-, or 2,7-dioxynaphthalene units and the bipyridinium units of the tetracationic cyclophane. Although Process I is without doubt happening, it could not be observed in the [2]catenanes $31 \cdot 4\text{PF}_6$ – $33 \cdot 4\text{PF}_6$ because only one translational isomer in each case could be detected by dynamic ^1H NMR spectroscopy. For [2]catenane $31 \cdot 4\text{PF}_6$, the coalescence of the signals corre-

sponding to the α protons on the bipyridinium units located inside and alongside the tetracationic cyclophane at 267 K is a consequence of Process II becoming fast on the ^1H NMR timescale. An energy barrier of $13.4\text{ kcal mol}^{-1}$ was calculated for this process. For the [2]catenanes $32 \cdot 4\text{PF}_6$ and $33 \cdot 4\text{PF}_6$, although some broadening of the ^1H NMR spectrum could be observed on cooling down the samples (an indication that Process II was happening), the temperature could not be reduced sufficiently for energy barriers for this process to be obtained.

Absorption spectra, luminescence properties, and intercomponent electronic interactions: These studies have been focused on the macrocyclic polyethers **5**, **19**, and **26** and their [2]catenanes 6^{4+} , 20^{4+} , and 30^{4+} . In order to elucidate the occurrence of intercomponent electronic interactions, it is necessary to compare the absorption and luminescence behavior of the macrocyclic polyethers and of their [2]catenanes with those of suitable model compounds. Therefore, we have investigated the absorption and luminescence properties of 1,4-dimethoxybenzene (1,4-DMB), 1,4-xylyl (1,4-Xyl), 2,6-dimethylnaphthalene (2,6-DMeN), and 1,5-dimethoxynaphthalene (1,5-DMN), which are good models for the aromatic units incorporated in the macrocyclic polyethers and corresponding catenanes. The absorption and luminescence properties of the model compounds, the macrocyclic polyethers, and the derived [2]catenanes are given in Table 1. The cyclophane 8^{4+} , which is a common component of the [2]catenanes examined in this paper, shows an absorption band with a maximum at 261 nm in MeCN solution, but no luminescence.^[20]

Macrocyclic polyether 5 and [2]catenane 6^{4+} : The absorption and fluorescence spectra in MeCN solution at room temperature of the chromophoric and luminescent moieties of the macrocyclic polyether **5** and of the model compounds 1,4-DMB and 1,4-Xyl are shown in Figure 1. The absorption spectrum of the macrocyclic polyether is different from the sum of the absorption spectra of its two components: the vibrational structure of the 1,4-Xyl around 270 nm is missing and the intensity in the band maximum is noticeably smaller. As shown in Figure 1 and Table 1, 1,4-DMB and 1,4-Xyl exhibit a strong fluorescence band in MeCN solution at room

Table 1. Table 1 Absorption and emission data.^[a]

	Absorption		Fluorescence RT			Fluorescence, 77 K		Phosphorescence 77 K	
	λ_{max} (nm)	ϵ ($\text{M}^{-1}\text{ cm}^{-1}$)	λ_{max} (nm)	τ (ns)	ϕ ^[b]	λ_{max} (nm)	τ (ns)	λ_{max} (nm)	τ (s)
1,4-DMB	290	2900	320	2.0	0.11	317 ^[c]	3.8 ^[c]	408 ^[c]	2.1 ^[c]
1,4-Xyl	267 ^[d]	410	293	9.3	0.08	288 ^[c]	32 ^[c]	396 ^[c]	7.2 ^[c]
1,5-DMN	294 ^[d]	8500	330 ^[d]	7	0.38	3.27 ^[d]	11	514 ^[d]	≈ 2
2,6-DMeN	237 ^[d]	4500	343 ^[d]	11.5	0.14	340 ^[c, d]	50 ^[c]	458 ^[c, d]	0.5 ^[c]
5	290	2200	325	2.2	0.09	317 ^[c]	4.1 ^[c]	412 ^[c]	2.2 ^[c]
6⁴⁺	263, 465	40 000, 430							
26	295 ^[d]	9000	345 ^[d]	8	0.30	327 ^[d]	14	483 ^[d]	1.8
30⁴⁺	265, 520	37 000, 520							
19	275	5700	340 ^[d] , 435 ^[e]	0.38, 10	0.004, 0.036 ^[f]	337 ^[c, d]	80 ^[c]	477 ^[c, d]	2.1 ^[c]
20⁴⁺	263, 440	35 000, 770							

[a] Air-equilibrated MeCN solution, unless otherwise noted; for errors, see experimental. [b] The standard used was naphthalene in degassed cyclohexane, $\phi = 0.23$ (see ref. [28]) unless otherwise noted. [c] Butyronitrile solution. [d] Structured band. [e] Exciplex-type emission, see text. [f] The standard used was quinine sulfate in H_2SO_4 1N, $\phi = 0.55$ (see ref. [29]).

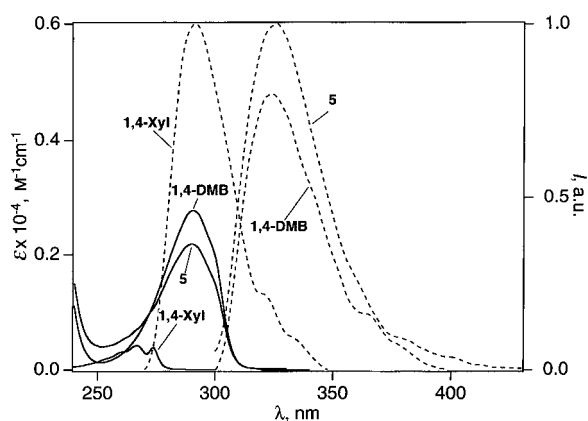


Figure 1. Absorption (unbroken lines) and emission (dashed lines) spectra of the macrocyclic polyether **5** and of the model compounds 1,4-DMB and 1,4-Xyl in MeCN solution at room temperature. For more details, see the text.

temperature. In the macrocyclic polyether **5**, the fluorescence band of the 1,4-dimethoxybenzene-type unit is present with almost the same lifetime and quantum yield as in the 1,4-DMB model compound, whereas there is no trace of the fluorescence band of the 1,4-xylyl-type component. The same is true for the fluorescence and phosphorescence spectra in a rigid butyronitrile matrix at 77 K (Table 1): the macrocyclic polyether **5** shows only the fluorescence and phosphorescence bands of its 1,4-dimethoxybenzene-type unit, regardless of the excitation wavelength. These results show that in the macrocyclic polyether the S_1 (and, if populated, T_1) level of the 1,4-xylyl-type unit is quenched by the lower-lying S_1 (and T_1) level of the 1,4-dimethoxybenzene-type unit, as schematized in Figure 2. Since the excitation spectrum of **5** ($\lambda_{em} = 330$ nm) coincides with the absorption spectrum throughout the entire spectral region, the quenching takes place by energy transfer^[16] from the 1,4-xylyl- to the 1,4-dimethoxybenzene-type unit.

The absorption spectrum (Figure 3) of the [2]catenane **6⁴⁺** is similar to the sum of the spectra of its **5** and **8⁴⁺** components in the UV region, but it shows a tail in the 310–400 nm region

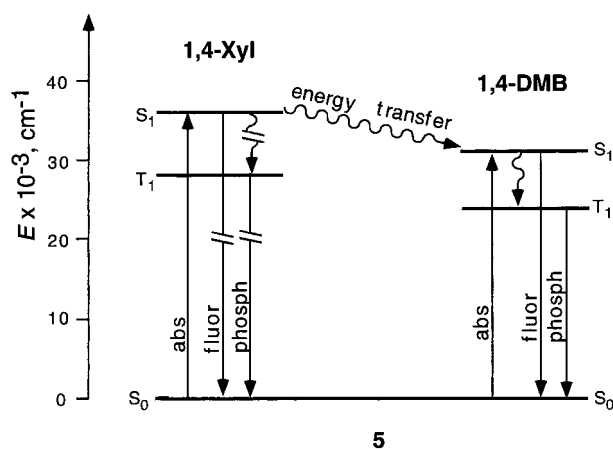


Figure 2. Schematic energy-level diagram for the macrocyclic polyether **5**. The energy levels of the S_1 and T_1 excited states have been evaluated from the onset of the emission spectra of the model compounds. Only the most relevant processes are shown.

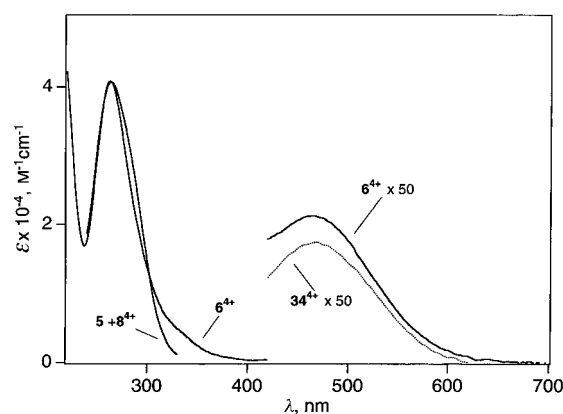
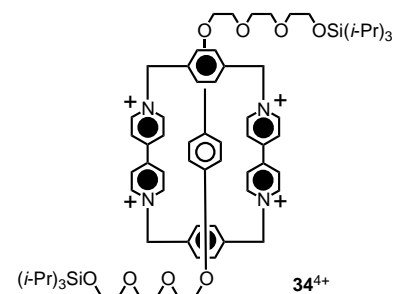


Figure 3. Absorption spectrum in MeCN solution of the [2]catenane **6⁴⁺** compared with the sum of the spectra of its **5** and **8⁴⁺** components. The dotted line shows the band in the visible region exhibited by the [2]rotaxane **34⁴⁺**, comprised of a 1,4-dimethoxybenzene-type unit surrounded by the tetracationic cyclophane.^[20]

and a new, broad absorption band in the visible region, with a maximum at 465 nm. Bands of this kind are found in the absorption spectra of all the catenanes and rotaxanes containing electron-donor and electron-acceptor units.^[14c, 20, 23] In particular, the [2]rotaxane **34⁴⁺**, containing a



1,4-dimethoxybenzene-type unit surrounded by the tetracationic cyclophane, shows a CT band of comparable intensity with $\lambda_{max} = 470$ nm (Figure 3).^[20] Therefore, this visible band of **6⁴⁺** can be assigned to a CT transition from the 1,4-dimethoxybenzene-type unit present in the macrocyclic polyether to the electron-acceptor bipyridinium units of the tetracationic cyclophane. The difference between the spectrum of **6⁴⁺** and the sum of the spectra of its two components shows the presence of another band at shorter wavelength ($\lambda_{max} \approx 330$ nm in Figure 3). This new band can be attributed to a CT transition from the 1,4-xylyl-type unit of the macrocyclic polyether, which is a worse electron donor than the 1,4-dimethoxybenzene-type unit, to the bipyridinium units of the tetracationic cyclophane.

As far as emission is concerned, it should be noted that in the spectrum of **6⁴⁺** the strong fluorescence bands of the 1,4-xylyl and 1,4-dimethoxybenzene-type units (the latter one still present in the emission spectrum of the macrocyclic polyether) are no longer observed (Table 1). This result can be accounted for by the presence, clearly shown by the absorption spectra (vide supra), of CT excited states lying below the potentially fluorescent levels of the two units, which offer a route to fast radiationless decay (Figure 4).

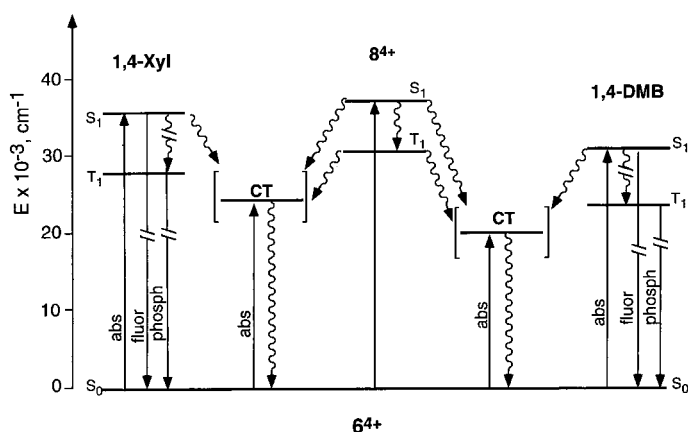


Figure 4. Schematic energy-level diagram for the [2]catenane 6^{4+} . Only the most relevant processes are shown.

Macrocyclic polyether 26 and [2]catenane 30^{4+} : The absorption and fluorescence spectra in MeCN solution at room temperature of the chromophoric and luminescent moieties of the macrocyclic polyether **26** and of the model compounds 1,4-Xyl and 1,5-DMN are shown in Figure 5. The absorption

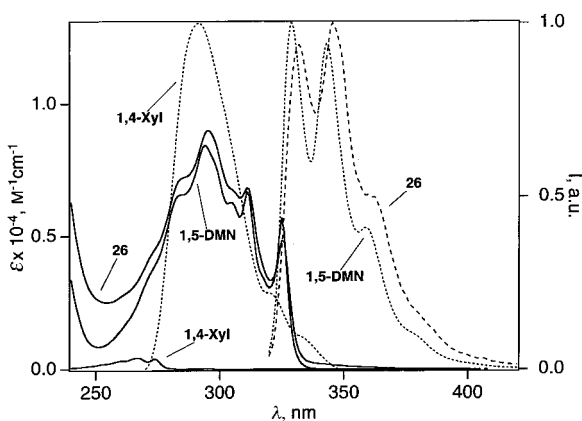


Figure 5. Absorption (unbroken lines) and emission (dashed lines) spectra of the macrocyclic polyether **26** and of the model compounds 1,4-Xyl and 1,5-DMN in MeCN solution at room temperature. For more details, see the text.

spectrum of the macrocyclic polyether is very similar to the sum of the absorption spectra of its two components. Both 1,4-Xyl and 1,5-DMN exhibit a strong fluorescence band in MeCN solution at room temperature (Figure 5 and Table 1). The macrocyclic polyether **26** shows an intense band with a maximum at 345 nm, which is very similar (also in structure, intensity, and lifetime) to the band exhibited by the 1,5-DMN model compound. No trace can be found of the fluorescence band of the *p*-xylyl component. The same is true for the fluorescence and phosphorescence spectra in a rigid butyronitrile matrix at 77 K (Table 1): the macrocyclic polyether **26** shows only the fluorescence and phosphorescence bands of its 1,5-dimethoxynaphthalene-type unit, regardless of the excitation wavelength. The excitation spectrum of **26** ($\lambda_{em} = 345$ nm) at room temperature coincides with the absorption spectrum throughout the entire spectral region. These results

indicate that in the macrocyclic polyether **26** the S_1 (and presumably the T_1) level of the 1,4-xylyl-type unit are quenched by energy transfer to the lower-lying S_1 (T_1) level of the 1,5-dimethoxynaphthalene-type unit (cf., macrocyclic polyether **5**, vide supra).

As in the case of the [2]catenane 6^{4+} , the absorption spectrum (Figure 6) of 30^{4+} shows an intense absorption tail in

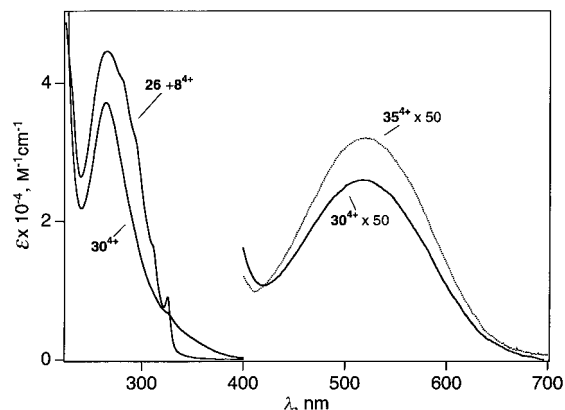
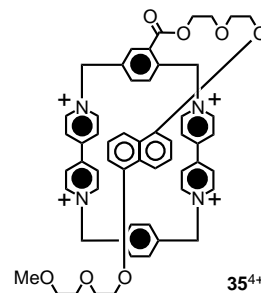


Figure 6. Absorption spectrum in MeCN solution of the [2]catenane 30^{4+} compared with the sum of the spectra of its **26** and 8^{4+} components. The dotted line shows the band in the visible region exhibited by tethered pseudorotaxane 35^{4+} , where a 1,5-dimethoxynaphthalene-type unit is enclosed in a tetracationic cyclophane.^[18d]

the 300–400 nm spectral region and a new absorption band in the visible region ($\lambda_{max} = 520$ nm), which are not present in the spectra of its macrocyclic polyether and tetracationic cyclophane components. The band with $\lambda_{max} = 520$ nm is very similar to that shown by the tethered pseudorotaxane 35^{4+} (Figure 6) in which a 1,5-dimethoxynaphthalene-type unit is enclosed within the tetracationic cyclophane.^[18d] Therefore, this band can be assigned to a CT transition from the 1,5-dimethoxynaphthalene-type unit present in the macrocyclic polyether to the electron-acceptor bipyridinium units of the tetracationic cyclophane. The difference between the spectrum of 30^{4+} and the sum of the spectra of its two components in the 300–400 nm region (Figure 6) shows the presence of another CT band with λ_{max} around 330 nm, as in the case of the [2]catenane 6^{4+} . Once again, this band can be attributed to a CT transition from the 1,4-xylyl-type unit of the macrocyclic polyether to the bipyridinium unit of the tetracationic cyclophane. The [2]catenane 30^{4+} does not exhibit any luminescence bands for the same reasons, previously discussed for 6^{4+} , that are related to the presence of low-energy, non-emitting CT levels.



Macrocyclic polyether 19 and [2]catenane 20^{4+} : The absorption and fluorescence spectra in MeCN solution at room temperature of the chromophoric and luminescent moieties of the macrocyclic polyether **19** and of the model compounds 1,4-DMB and 2,6-DMeN are shown in Figure 7. The absorp-

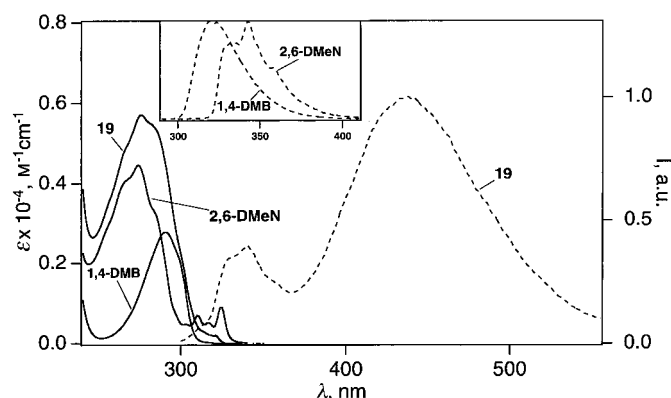


Figure 7. Absorption (unbroken lines) and emission (dashed lines) spectra in MeCN solution at room temperature of the macrocyclic polyether **19** and of the model compounds 1,4-DMB and 2,6-DMeN. The emission spectra of the two model compounds are given in an inset for clarity. For more details, see the text.

tion spectrum of the macrocyclic polyether is different from the sum of the absorption spectra of its two components since the structure of the 1L_b ($\pi-\pi^*$) band of 2,6-DMeN in the 310–330 nm region^[24] is missing. This difference could arise from electronic intercomponent interactions or physical constraints imposed upon the chromophoric group by the macrocyclic structure. As shown in the right-hand part of Figure 7 (see also Table 1), in MeCN solution at room temperature, the macrocyclic polyether **19** has two emission bands: a weak, short-lived, and structured band with a maximum at 340 nm, and a more intense, relatively long-lived, broad band with a maximum at 435 nm. Comparison with the emission spectra of the 1,4-DMB and 2,6-DMeN model compounds (Figure 7, inset) shows that the fluorescence band of the 1,4-dimethoxybenzene-type unit is almost completely missing (its intensity is $<0.1\%$ of that shown by 1,4-DMB), and that of the 2,6-dimethylnaphthalene-type unit is about 40 times weaker than in the 2,6-DMeN model compound (a parallel decrease in the fluorescence lifetime is also observed, Table 1) regardless of the excitation wavelength. The broad band with maximum at 435 nm, which is not present in the spectra of the components, must result from an intercomponent interaction between the two chromophoric units. The most likely hypothesis is the presence of a CT (or exciplex-type) excited state involving the 1,4-dimethoxybenzene-type unit as an electron donor and the naphthalene moiety as an electron acceptor. The excitation spectrum matches the absorption spectrum in the entire spectral region both at $\lambda_{em} = 330$ nm (emission of the 2,6-dimethylnaphthalene-type unit) and at $\lambda_{em} = 440$ nm (new emission band). This result indicates that excitation of the 1,4-dimethoxybenzene-type unit is followed by a very efficient energy transfer to the fluorescent level of the 2,6-dimethylnaphthalene-type unit, which then partially deactivates to the lower-lying interchromophoric CT level. In a rigid butyronitrile matrix at 77 K, the macrocyclic polyether **19** shows only the fluorescence and phosphorescence bands of its 2,6-dimethylnaphthalene-type unit, an indication that, under such conditions, there is no low-energy interchromophoric CT level, presumably because of constraints imposed by the rigid matrix on the intra-

molecular movements and/or the lack of solvent reorganization.

The presence of interchromophoric interactions in **19** has been investigated in more detail. On going from MeCN to CH_2Cl_2 solution, the emission maximum at 435 nm undergoes a blue shift, as expected on account of the destabilization of CT-type excited states on decreasing the dielectric constant of the solvent. In MeCN solution, addition of CF_3COOH or NH_4PF_6 causes a decrease in the intensity of the 435 nm band; this indicates that when the oxygen atoms of the macrocyclic polyether are engaged in hydrogen bonding the intercomponent electronic interaction is, at least in part, prevented. The metal complex $[\text{Pt}(\text{bpy})_2(\text{NH}_3)_2]^{2+}$ (bpy = 2,2'-bipyridine), which is known to give adducts with aromatic macrocyclic polyethers,^[25, 26] can be dissolved in CH_2Cl_2 only in the presence of **19**. Figure 8 shows the absorption spectrum of

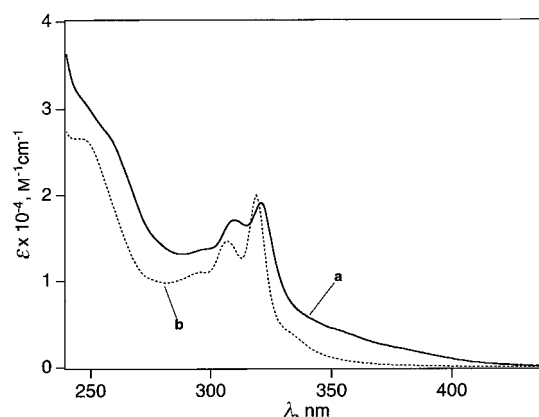


Figure 8. Absorption spectrum in CH_2Cl_2 solution of the adduct between the macrocyclic polyether **19** and $[\text{Pt}(\text{bpy})_2(\text{NH}_3)_2]^{2+}$ (a) compared with the sum of the spectra of the two components (b).

the adduct, which exhibits an intense tail above 330 nm, indicative of a CT transition from the electron-donor units of the macrocyclic polyether to the electron deficient 2,2'-bipyridine ligand of the complex.^[25] In the adduct, neither the residual fluorescence of the S_1 excited state of the 2,6-dimethylnaphthalene-type moiety ($\lambda_{max} = 340$ nm), nor the CT-type emission ($\lambda_{max} = 435$ nm) of free macrocyclic polyether **19** (Figure 7) are observed. As in the case of $[\text{Pt}(\text{bpy})_2(\text{NH}_3)_2]^{2+}$ adducts with other macrocyclic hosts, it is likely that the flat metal complex intercalates between the two aromatic moieties of the macrocyclic polyether. This $\pi-\pi$ stacking interaction would i) prevent intercomponent electronic interactions between the two chromophoric moieties and ii) result in the presence of low-energy CT excited states^[25, 26] capable of deactivating the upper-lying luminescent levels.

As in the case of the [2]catenanes **6**⁴⁺ and **30**⁴⁺, the absorption spectrum of the [2]catenane **20**⁴⁺ shows a tail in the 310–400 nm region (Figure 9) and a new, broad absorption band in the visible region with a maximum at 440 nm not present in the spectra of its macrocyclic polyether and tetracationic components. This band can be assigned to CT transitions from the electron-donor units present in the macrocyclic polyether to the electron-acceptor bipyridinium

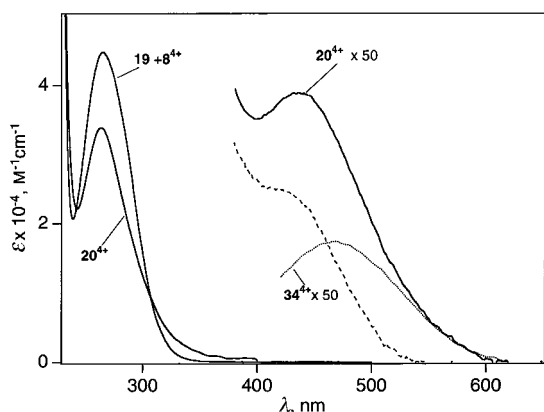


Figure 9. Absorption spectrum in MeCN solution of the [2]catenane 20^{4+} compared with the sum of the spectra of its 19 and 8^{4+} components. The dotted line shows the band in the visible region exhibited by the [2]rotaxane 34^{4+} . The dashed line shows the difference between the spectra of 20^{4+} and 34^{4+} .

units of the tetracationic cyclophane. The broad CT band can be deconvoluted into two components, one ($\lambda_{\max} = 470$ nm)^[20] corresponding to that previously found in the rotaxane 34^{4+} and the other one with $\lambda_{\max} = 430$ nm. The latter band can be attributed to a CT transition involving the 2,6-dimethylnaphthalene-type unit of the macrocyclic polyether, which is a worse electron donor than the 1,4-dimethoxybenzene-type unit. Considering the intense tail of the UV band, the intensity of the 470 nm band appears to be larger than that of the 430 nm band.

As in the case of 6^{4+} and 30^{4+} , 20^{4+} does not exhibit any luminescence bands. This result is expected because of the previously discussed presence of low-energy CT excited states below the fluorescent levels of the component units. It should also be noted that interactions between the two chromophoric moieties of the macrocyclic polyether are impossible in the [2]catenane, because of the interposed bipyridinium unit of the tetracationic cyclophane.

Conclusions

The nature of the aromatic units in the macrocyclic polyether has been shown to have a dramatic effect on i) the efficiency of the catenation with $8 \cdot 4PF_6$, ii) ratios of translational isomers, and iii) the dynamic processes occurring in the [2]catenanes.

- Replacement of the phenolic oxygen atoms by methylene groups in the hydroquinone ring greatly reduces the recognition between the aromatic ring and the tetracationic cyclophane.
- The *p*-xylyl and 1,5-dioxynaphthalene units compete for inclusion within the cavity of the tetracationic cyclophane. In each of the three [2]catenanes incorporating a macrocyclic polyether containing a *p*-xylyl unit and either the 1,6-, 2,6-, or 2,7-dioxynaphthalene units, only the *p*-xylyl unit is located inside the tetracationic cyclophane.
- The macrocyclic polyethers **5**, **19**, and **26**, which contain two different aromatic moieties, and their [2]catenanes 6^{4+} , 20^{4+} , and 30^{4+} exhibit interesting UV/Vis and luminescence

properties. Comparison with the behavior of simple model compounds has shown the presence of electronic interactions causing energy-transfer processes between the aromatic units of the macrocyclic polyethers and CT processes in the [2]catenanes.

This investigation has demonstrated how subtle changes in the stereoelectronic information imprinted within the molecular components of a series of [2]catenanes can dramatically affect the efficiency of the self-assembly process, as well as influencing the molecular recognition and electronic interactions within the resulting structures.

Experimental Section

General methods: Solvents were dried where necessary by literature methods.^[27] NaH was used as a 60% dispersion in mineral oil, which was not removed before use. Thin-layer chromatography was performed on aluminum plates pre-coated with Merck 5735 silica gel 60 F₂₅₄. Plates were air-dried and scrutinized under a UV lamp. Column chromatography was performed with silica gel 60 (particle size 0.040–0.063 mm, Merck 9385). Melting points were determined with an Electrothermal 9200 melting point apparatus and are uncorrected. Mass spectra were obtained from Kratos MS25 or Profile instruments, the latter being equipped with a FAB facility (with a krypton or xenon primary atom beam in conjunction with a 3-nitrobenzyl alcohol matrix). Positive-ion electrospray mass spectra were recorded on either a VG Quattro triple quadrupole mass spectrometer, or a VG Platform single quadrupole instrument. ¹H NMR spectra were recorded on Bruker AC250 (250 MHz), AC300 (300 MHz), AMX360 (360 MHz), AMX400 (400 MHz), or AMX500 (500 MHz) (with the deuterated solvent as the lock and residual solvent or TMS as the internal reference) spectrometers. ¹³C NMR spectra were recorded on Bruker AC300 (75 MHz), or AC360 (90 MHz) spectrometers. Microanalyses were performed by the University of Birmingham and by the University of North London Microanalytical Services.

α,α' -Bis[2-[2-[2-(2-hydroxyethoxy)ethoxy]ethoxy]ethoxy]-*p*-xylylene (10**):** 1,4-Bis(bromomethyl)benzene (10.0 g, 37.9 mmol) was added to a suspension of NaH (6.06 g, 151.5 mmol) in tetraethylene glycol (200 mL) under N_2 and stirred for 48 h at 40 °C. After this had cooled down to room temperature, H_2O (500 mL) was added, and the solution extracted with Et_2O (100 mL) and CH_2Cl_2 (3×150 mL). The CH_2Cl_2 layers were combined, washed with H_2O (3×30 mL), and dried ($MgSO_4$), and the solvent removed. The residue was purified by column chromatography (SiO_2 , $CH_2Cl_2/MeOH$ 20:1) to yield **10** as a colorless oil (13.10 g, 71%). ¹H NMR (300 MHz, $CDCl_3$): $\delta = 7.33$ (s, 4H), 4.56 (s, 4H), 3.58–3.74 (m, 32H), 2.72 (brs, 2H); ¹³C NMR ($CDCl_3$, 75 MHz): $\delta = 137.6$, 127.8, 73.0, 70.6, 70.6, 70.6, 70.6, 70.6, 70.3, 69.4, 61.7; MS (FAB): m/z (%) = 491 (36) [$M^+ + H$].

α,α' -Bis[2-[2-[2-(*p*-toluenesulfonyl)ethoxy]ethoxy]ethoxy]-*p*-xylylene (21**):** The diol **10** (17.5 g, 35.6 mmol) was dissolved in CH_2Cl_2 (250 mL) along with Et_3N (7.2 g, 71.3 mmol) and 4-(dimethylamino)pyridine (cat.) and cooled to 0 °C. A solution of *p*-toluenesulfonyl chloride (13.6 g, 71.3 mmol) in CH_2Cl_2 (150 mL) was added during 1 h and the reaction stirred overnight. The solution was washed with 5% aqueous HCl (2×200 mL) and H_2O (200 mL), and dried ($MgSO_4$). The solution was concentrated and the residue purified by column chromatography (SiO_2 , $CH_2Cl_2/MeOH$ 50:1) to yield **21** as a colorless oil (26.00 g, 91%). ¹H NMR ($CDCl_3$, 300 MHz): $\delta = 7.78$ (d, $J = 8.0$ Hz, 4H), 7.32 (d, $J = 8.0$ Hz, 4H), 7.28 (s, 4H), 4.53 (s, 4H), 3.54–3.69 (m, 32H), 2.42 (s, 6H); ¹³C NMR ($CDCl_3$, 75 MHz): $\delta = 144.9$, 137.7, 133.0, 129.9, 127.9, 127.8, 72.9, 70.6, 70.6, 70.5, 70.5, 69.4, 69.4, 68.6, 21.6; MS (FAB): m/z (%) = 799 (13) [$M^+ + H$]; $C_{38}H_{54}O_{14}S_2$ (798): calcd C 57.13, H 6.81; found C 57.50, H 6.96.

***p*-Phenylene-*p*-xylyl-36-crown-10 (**5**):** Hydroquinone (0.97 g, 8.81 mmol) in dry DMF (100 mL) and **21** (7.00 g, 8.77 mmol) in dry DMF (100 mL) were added to a stirred slurry of Cs_2CO_3 (55.3 g, 0.170 mol) in dry DMF (600 mL) under N_2 . The reaction was stirred at 70 °C for 5 d and then cooled down to room temperature and filtered. The solvent was removed to give a brown solid, which was dissolved in PhMe (200 mL) and washed with

H₂O (200 mL). The aqueous layer was extracted with PhMe (3 × 100 mL) and the combined organic extracts were dried (MgSO₄). The solution was concentrated to give a brown oil which was purified by column chromatography (SiO₂, acetone/hexane 7:5) to yield **5** as a clear colorless oil (1.12 g, 23%). ¹H NMR (300 MHz, CDCl₃, 298 K): δ = 7.27 (s, 4H), 6.80 (s, 4H), 4.51 (s, 4H), 4.02–4.06 (m, 4H), 3.80–3.84 (m, 4H), 3.63–3.73 (m, 20H), 3.55–3.65 (m, 4H); ¹³C NMR (75 MHz, CDCl₃): δ = 153.2, 137.7, 127.7, 115.7, 73.0, 70.9, 70.8, 70.7, 70.7, 69.8, 69.6, 68.3; MS (FAB): *m/z* (%) = 564 (46) [*M*⁺]; C₃₀H₄₄O₁₀ (564): calcd C 63.81, H 7.85; found C 63.81, H 7.68.

Bis-*p*-xylyl-38-crown-10 (11): A solution of 1,4-bis(bromomethyl)benzene (6.00 g, 22.7 mmol) and tetraethylene glycol (4.40 g, 22.7 mmol) in dry THF (300 mL) was added over 48 h to a refluxing suspension of NaH (2.3 g, 56.8 mmol) in dry THF (300 mL) under N₂ with stirring, and heated under reflux for 24 h. After cooling down to room temperature, H₂O (20 mL) was added and the solvent removed to yield an oily residue which was dissolved in PhMe (200 mL) and washed with aqueous 0.1M HCl (200 mL). The aqueous solution was extracted with PhMe (2 × 100 mL), the combined organic layers were dried (MgSO₄), and the solution concentrated. The resulting pale oil was purified by column chromatography (SiO₂, CH₂COCH₃/hexane 5:7) to yield **11** as a colorless oil (500 mg, 4%). ¹H NMR (300 MHz, CD₃COCD₃): δ = 7.32 (s, 8H), 4.51 (s, 8H), 3.58 (m, 32H); ¹³C NMR (75 MHz, CD₃COCD₃): δ = 139.4, 128.1, 73.1, 71.3, 71.2, 70.3; MS (FAB): *m/z* (%) = 591 (6) [*M*⁺+H]; C₃₂H₄₈O₁₀ (592): calcd C 64.84, H 8.16; found: C 64.60, H 8.40.

34-Crown-8 derivative (15): A solution of **13** (4.50 g, 6.60 mmol) in dry THF (200 mL) was added over 15 min to a refluxing suspension of 1,4-phenylene dipropanol (**14**) (1.28 g, 6.60 mmol) and NaH (0.79 g, 19.79 mmol) in dry THF (400 mL) under N₂, and the solution was heated under reflux for 4 d. The reaction was cooled down to room temperature and quenched with H₂O, and the solution was concentrated. The residue was dissolved in CH₂Cl₂ (150 mL), washed with H₂O (3 × 100 mL), and dried (MgSO₄). The solvent was removed and the residue purified by column chromatography (SiO₂, CH₂Cl₂/MeOH 100:1) to yield **15** as a white crystalline solid (1.20 g, 34%). M.p.: 42.0–42.5 °C; ¹H NMR (300 MHz, CDCl₃): δ = 7.06 (s, 4H), 6.78 (s, 4H), 4.03 (t, 4H), 3.83 (t, 4H), 3.62–3.76 (m, 12H), 3.59 (t, 4H), 3.47 (t, 4H), 2.64 (t, 4H), 1.85 (m, 4H); ¹³C NMR (CD₃COCD₃, 75 MHz): δ = 153.3, 139.5, 128.6, 115.8, 71.0, 71.0, 70.9, 70.5, 70.3, 70.0, 68.4, 32.0, 31.6; MS (FAB): *m/z* (%) = 532 (100) [*M*⁺]; HRMS calcd for [*M*⁺] C₃₀H₄₄O₈ 532.3036, found 532.3038.

Naphthalene-2,6-dimethyl-*p*-phenylene-38-crown-10 (19): The procedure for the preparation of **5** was followed, with **17** (6.00 g, 7.07 mmol), hydroquinone (0.78 g, 7.10 mmol), and Cs₂CO₃ (44.6 g, 0.137 mol) to yield colorless crystals of **19** (0.77 g, 18%). M.p.: 61.5–62.0 °C; ¹H NMR (300 MHz, CDCl₃, 298 K): δ = 7.77 (d, *J* = 8.0 Hz, 2H), 7.73 (brs, 2H), 7.44 (dd, *J* = 1.5, 8.0 Hz, *J* = 1.5 Hz, 2H), 6.69 (s, 4H), 4.71 (s, 4H), 3.92–3.96 (m, 4H), 3.76–3.82 (m, 4H), 3.64–3.74 (m, 24H); ¹³C NMR (CDCl₃, 75 MHz): δ = 153.2, 135.9, 128.1, 132.8, 126.1, 126.0, 115.5, 73.3, 70.8, 70.8, 70.8, 70.8, 69.7, 69.6, 68.1; MS (FAB): *m/z* (%) = 614 (100) [*M*⁺]; C₃₄H₄₆O₁₀ (614): calcd C 66.43, H 7.54; found C 66.73, H 7.51.

1,5-Naphtho-*p*-xylyl-38-crown-10 (26): 1,5-Dihydroxynaphthalene (0.80 g, 5.01 mmol) was added to a previously degassed suspension of Cs₂CO₃ (32.7 g, 100 mmol) and CsOTs (1.53 g, 5.01 mmol) in dry DMF (400 mL) under N₂. After stirring for 1 h at 80 °C, a solution of **20** (4.00 g, 5.01 mmol) and CsOTs (1.53 g, 5.01 mmol) in dry, degassed DMF (200 mL) was added over 1 h and the heating was maintained for 5 d. After cooling down to room temperature, the reaction mixture was filtered. The filtrate was collected and the solvent removed to leave a solid residue, which was dissolved in PhMe (200 mL) and washed with H₂O (250 mL). The aqueous layer was washed with PhMe (3 × 100 mL). The organic layers were combined and dried (MgSO₄), and the solution was concentrated. The resulting brown oil was purified by column chromatography (SiO₂, CH₂Cl₂/MeOH 100:2), followed by recrystallization (CHCl₃/hexane) to yield **26** as a white crystalline solid (1.50 g, 52%). M.p.: 104.0–104.5 °C; ¹H NMR (300 MHz, CDCl₃): δ = 7.86 (d, *J* = 8.0 Hz, 2H), 7.30 (d, *J* = 8.0 Hz, 2H), 7.18 (s, 4H), 6.79 (d, *J* = 8.0 Hz, 2H), 4.39 (s, 4H), 4.26 (t, 4H), 3.79 (t, 4H), 3.56–3.73 (m, 16H), 3.46 (t, 4H); ¹³C NMR (CDCl₃, 75 MHz): δ = 154.4, 137.6, 127.6, 126.9, 125.1, 114.7, 105.8, 72.9, 71.1, 70.9, 70.9, 70.7, 70.6, 69.8, 69.5, 68.1; MS (FAB): *m/z* (%) = 614 (100) [*M*⁺]; C₃₄H₄₆O₁₀ (608): calcd C 66.42, H 7.54; found C 66.12, H 7.76.

1,6-Naphtho-*p*-xylyl-37-crown-10 (27): The procedure described for the preparation of **26**, with 1,6-dihydroxynaphthalene, was followed to give **27** as a white crystalline solid (0.69 g, 33%). M.p.: 96.0–97.0 °C; ¹H NMR (CDCl₃, 300 MHz): δ = 8.18 (d, *J* = 11.3 Hz, 1H), 7.99 (s, 1H), 7.25 (m, 6H), 7.07 (d, *J* = 4.0 Hz, 1H), 6.65 (dd, *J* = 2.5, 9.0 Hz, 1H), 4.45 (s, 2H), 4.40 (s, 2H), 4.25 (t, 2H), 4.19 (t, 2H), 3.95 (t, 2H), 3.88 (t, 2H), 3.44–3.80 (m, 24H); ¹³C NMR (75 MHz, CDCl₃): δ = 157.5, 154.9, 137.8, 136.0, 127.9, 127.9, 126.7, 124.1, 121.2, 119.6, 118.0, 106.8, 103.2, 73.0, 71.3, 71.1, 70.9, 70.9, 70.0, 69.9, 69.5, 68.1, 67.7; MS (FAB): *m/z* (%) = 614 (100) [*M*⁺]; C₃₄H₄₆O₁₀ (614): calcd C 66.43, H 7.54; found C 66.61, H 7.51.

2,6-Naphtho-*p*-xylyl-38-crown-10 (28): The procedure described for the preparation of **26**, with 2,6-dihydroxynaphthalene, was followed to give **28** as a white crystalline solid (1.62 g, 53%). M.p.: 98.0–98.5 °C; ¹H NMR (300 MHz, CDCl₃): δ = 7.56 (d, *J* = 15.0 Hz, 2H), 7.17 (s, 4H), 7.13 (dd, *J* = 2.5, 9.0 Hz, 2H), 7.08 (d, *J* = 2.5 Hz, 2H), 4.37 (s, 4H), 4.20 (t, 4H), 3.92 (t, 4H), 3.73 (t, 4H), 3.54–3.70 (m, 16H), 3.45 (t, 4H); ¹³C NMR (75 MHz, CDCl₃): δ = 155.4, 137.6, 129.8, 128.2, 127.6, 119.3, 107.5, 72.9, 71.0, 70.9, 70.8, 70.7, 70.6, 69.8, 69.5, 67.8; MS (FAB): *m/z* (%) = 614 (100) [*M*⁺]; C₃₄H₄₆O₁₀ (614): calcd C 66.43, H 7.54; found C 66.56, H 7.41.

2,7-Naphtho-*p*-xylyl-37-crown-10 (29): The procedure described for the preparation of **26**, with 2,7-dihydroxynaphthalene, was followed to give **29** as a white crystalline solid (0.28 g, 12%). M.p.: 102.0–102.5 °C; ¹H NMR (300 MHz, CDCl₃): δ = 7.62 (d, *J* = 9.0 Hz, 2H), 7.29 (s, 4H), 7.01 (m, 4H), 4.53 (s, 4H), 4.23 (t, 4H), 3.90 (t, 4H), 3.50–3.80 (m, 24H); ¹³C NMR (CDCl₃, 75 MHz): δ = 157.4, 137.7, 135.8, 129.1, 127.6, 124.5, 116.4, 106.4, 72.9, 70.9, 70.9, 70.8, 70.7, 70.7, 69.7, 69.5, 67.4; MS (FAB): *m/z* (%) = 637 (100) [*M*⁺+Na], 614 (24) [*M*⁺]; C₃₄H₄₆O₁₀ (614): calcd C 66.42, H 7.54; found C 66.26, H 7.48.

[2]Catenane 6·4PF₆: A solution of **5** (0.20 g, 0.355 mmol), **1**·2PF₆ (125 mg, 0.177 mmol) and **2** (52 mg, 0.195 mmol) in dry MeCN (7 mL) was stirred for 6 d in a sealed flask. The solvent was removed and the residue purified by column chromatography (SiO₂, MeOH/2M NH₄Cl/MeNO₂ 7:2:1). Counterion exchange (NH₄PF₆/H₂O) afforded **6·4PF₆** as a red solid (139 mg, 47%). M.p.: >250 °C; ¹H NMR (300 MHz, CD₃CN, 233 K): δ = 8.85 (m, 8H), 7.79 (m, 8H), 7.61 (m, 8H), 6.62 (s, 2.48H), 6.22 (s, 1.52H), 5.68 (s, 1.52H), 5.66 (s, 2.48H), 4.02 (s, 4H), 3.41 (s, 2.48H), 3.58 (s, 1.52H), 3.50–3.99 (m, 32H); ¹³C NMR (75 MHz, CD₃CN): δ = 155.3, 150.7, 149.5, 141.9, 141.6, 137.0, 136.1, 133.0, 130.8, 130.5, 129.8, 118.1, 77.0, 76.2, 76.1, 75.8, 75.2, 75.1, 74.9, 71.9, 70.0, 66.4; MS (FAB): *m/z* (%) = 1664 (1) [*M*⁺], 1519 (17) [*M*⁺ – PF₆], 1374 (21) [*M*⁺ – 2PF₆], 1229 (4) [*M*⁺ – 3PF₆]; C₆₆H₇₆F₂₄N₄O₁₀P₄ (1664): calcd C 47.60, H 4.60, N 3.36; found: C 47.36, H 4.40, N 3.11.

[2]Catenane 12·4PF₆: A solution of **11** (360 mg, 0.61 mmol), **1**·2PF₆ (210 mg, 0.31 mmol) and **2** (90 mg, 0.34 mmol) in dry MeCN (7 mL) was stirred for 5 d. The reaction was worked up as described for **6·4PF₆** to yield **11·4PF₆** as a pale yellow solid (200 mg, 38%). M.p.: >250 °C; ¹H NMR (400 MHz, CD₃CN, 333 K): δ = 8.86 (d, 8H), 7.79 (d, *J* = 7.0 Hz, 8H), 7.73 (s, 8H), 5.71 (s, 8H), 5.51 (brs, 8H), 3.97 (s, 8H), 3.76–3.90 (m, 32H); ¹³C NMR (75 MHz, CD₃CN): δ = 147.3, 145.6, 138.1, 137.9, 131.7, 128.0, 127.7, 72.8, 71.2, 65.7; MS (FAB): *m/z* (%) = 1547 (11) [*M*⁺ – PF₆], 1403 (5) [*M*⁺+H – 2PF₆]; C₆₈H₈₀F₂₄N₄O₁₀P₄ (1692): calcd C 48.23, H 4.76, N 3.31; found: C 47.93, H 4.77, N 3.50.

[2]Catenane 16·4PF₆: A solution of **15** (250 mg, 0.47 mmol), **1**·2PF₆ (133 mg, 0.19 mmol) and **2** (55 mg, 0.21 mmol) in dry MeCN (7 mL) was stirred for 5 d. The reaction was worked up as described for **6·4PF₆** to yield **16·4PF₆** as an orange/red solid (34 mg, 11%). M.p.: >250 °C; ¹H NMR (400 MHz, CD₃COCD₃, 298 K): δ = 9.35 (d, 8H), 8.26 (d, 8H), 8.08 (s, 8H), 6.59 (s, 4H), 6.04 (s, 8H), 3.70–4.03 (m, 32H), 3.27 (t, 4H); ¹³C NMR (100 MHz, CD₃COCD₃): δ = 151.1, 147.6, 146.1, 139.6, 137.8, 131.9, 128.6, 126.8, 114.0, 71.7, 71.5, 71.0, 70.9, 70.8, 69.3, 67.4, 65.7, 31.6, 31.5; MS (FAB): *m/z* (%) = 1487 (13) [*M*⁺ – PF₆], 1342 (27) [*M*⁺ – 2PF₆], 1197 (6) [*M*⁺ – 3PF₆]; HRMS calcd for [*M*⁺ – PF₆] C₆₈H₈₀F₁₈N₄O₁₀P₃ 1487.4589, found 1487.4624.

[2]Catenane 20·4PF₆: A solution of **19** (230 mg, 0.38 mmol), **1**·2PF₆ (115 mg, 0.16 mmol) and **2** (48 mg, 0.18 mmol) in dry MeCN (7 mL) was stirred for 5 d. The reaction was worked up as described for **6·4PF₆** to yield **20·4PF₆** as an orange/red solid (125 mg, 45%). M.p.: >250 °C; ¹H NMR (300 MHz, CD₃CN, 343 K): δ = 8.77 (d, *J* = 7.0 Hz, 8H), 7.79 (s, 8H), 7.44 (d, *J* = 7.0 Hz, 8H), 7.20 (d, *J* = 7.9 Hz, 2H), 7.11 (d, *J* = 8.0 Hz, 2H), 7.07 (brs, 2H), 5.70 (s, 8H), 4.37 (s, 4H), 3.72–3.99 (m, 28H), 3.70 (s, 4H), 3.47 (m,

4H); ^{13}C NMR (CD_3CN , 75 MHz): $\delta = 155.3, 150.7, 149.5, 141.9, 141.6, 137.0, 136.1, 133.0, 130.8, 130.5, 129.8, 118.1, 77.0, 76.2, 76.1, 75.8, 75.2, 75.1, 74.9, 71.9, 70.0, 66.4$; MS (FAB): m/z (%) = 1569 (13) $[M^+ - \text{PF}_6^-]$, 1424 (28) $[M^+ - 2\text{PF}_6^-]$, 1279 (8) $[M^+ - 3\text{PF}_6^-]$; $\text{C}_{70}\text{H}_{78}\text{F}_{24}\text{N}_4\text{O}_{10}\text{P}_4$ (1714): calcd C 49.01, H 4.58, N 3.27; found: C 48.71, H 4.70, N 3.44.

[2]Catenane 30·4PF₆: A solution of **26** (225 mg, 0.38 mmol), **1**·2PF₆ (104 mg, 0.15 mmol) and **2** (43 mg, 0.16 mmol) in dry MeCN (7 mL) was stirred for 5 d. The reaction was worked up as described for **6**·4PF₆ to yield **30**·4PF₆ as a purple solid (130 mg, 52%). M.p.: >250 °C; ^1H NMR (400 MHz, CD_3CN , 278 K): $\delta = 8.51\text{--}8.89$ (m, 8H), 7.75–8.03 (m, 8H), 7.08–7.38 (m, 8H), 5.61–5.91 (m, 8H), 6.62 (s), 6.48 (d), 6.19 (d), 3.63 (brs), 3.36–4.24 (m, 40H); ^{13}C NMR (CD_3CN , 75 MHz) broad at room temperature; MS (FAB): m/z (%) = 1714 (2) $[M^+]$, 1570 (20) $[M^+ + \text{H} - \text{PF}_6^-]$, 1425 (16) $[M^+ + \text{H} - 2\text{PF}_6^-]$, 1297 (6) $[M^+ + \text{NH}_4 - 3\text{PF}_6^-]$; $\text{C}_{70}\text{H}_{78}\text{F}_{24}\text{N}_4\text{O}_{10}\text{P}_4$ (1714): calcd C 49.01, H 4.58, N 3.27; found: C 48.71, H 4.28, N 3.53.

[2]Catenane 31·4PF₆: A solution of **27** (262 mg, 0.43 mmol), **1**·2PF₆ (121 mg, 0.17 mmol) and **2** (50 mg, 0.19 mmol) in dry MeCN (7 mL) was stirred for 5 d. The reaction was worked up as described for **6**·4PF₆ to yield **31**·4PF₆ as a red solid (121 mg, 41%). M.p.: >250 °C; ^1H NMR (400 MHz, CD_3COCD_3 , 203 K): $\delta = 9.26$ (m, 8H), 8.04 (m, 8H), 7.73 (s, 8H), 8.03 (s, 8H), 7.38 (d, $J = 9.3$ Hz, 1H), 7.36 (t, $J = 7.9$ Hz, 1H), 7.11 (d, $J = 8.4$ Hz, 1H), 6.85 (d, $J = 7.7$ Hz, 1H), 6.71 (d, $J = 1.7$ Hz, 1H), 6.52 (dd, $^3J = 9.2$ Hz, 1H), 6.02 (s, 8H), 3.48–4.06 (m, 36H); ^{13}C NMR (75 MHz, CD_3CN): $\delta = 155.6, 146.6, 145.2, 138.2, 135.7, 131.5, 130.0, 129.1, 126.8, 119.7, 107.4, 72.1, 71.8, 71.4, 71.0, 70.7, 70.6, 69.9, 68.3$; MS (FAB): m/z (%) = 1715 (2) $[M^+ + \text{H}]$, 1570 (18) $[M^+ + \text{H} - 2\text{PF}_6^-]$, 1425 (23) $[M^+ + \text{H} - 3\text{PF}_6^-]$, 1280 (5) $[M^+ + \text{H} - 4\text{PF}_6^-]$; $\text{C}_{70}\text{H}_{78}\text{F}_{24}\text{N}_4\text{O}_{10}\text{P}_4$ (1714): calcd C 49.01, H 4.58, N 3.27; found: C 49.08, H 4.66, N 3.26.

[2]Catenane 32·4PF₆: A solution of **28** (300 mg, 0.49 mmol), **1**·2PF₆ (140 mg, 0.20 mmol) and **2** (60 mg, 0.21 mmol) in dry MeCN (7 mL) was stirred for 5 d. The reaction was worked up as described for **6**·4PF₆ to yield **32**·4PF₆ as a purple solid (145 mg, 42%). M.p.: >250 °C; ^1H NMR (CD_3CN , 400 MHz, 343 K): $\delta = 8.73$ (d, 8H), 7.80 (s, 8H), 7.53 (d, 8H), 7.14 (d, $J = 8.4$ Hz, 2H), 6.82 (d, $J = 8.4$ Hz, 2H), 6.41 (s, 2H), 5.71 (s, 8H), 4.05 (s, 4H), 3.62–3.90 (m, 36H); ^{13}C NMR (CD_3CN , 75 MHz): $\delta = 155.9, 146.3, 145.2, 137.8, 136.2, 131.5, 129.9, 129.1, 126.8, 119.7, 107.6, 72.1, 71.8, 71.4, 71.0, 70.8, 70.6, 70.0, 68.4, 65.4$; MS (FAB): m/z (%) = 1714 (2) $[M^+]$, 1569 (10) $[M^+ - \text{PF}_6^-]$, 1424 (11) $[M^+ - 2\text{PF}_6^-]$, 1279 (2) $[M^+ - 3\text{PF}_6^-]$; $\text{C}_{70}\text{H}_{78}\text{F}_{24}\text{N}_4\text{O}_{10}\text{P}_4$ (1714): calcd C 49.01, H 4.58, N 3.27; found: C 48.81, H 4.53, N 3.31.

[2]Catenane 33·4PF₆: A solution of **29** (148 mg, 0.24 mmol), **1**·2PF₆ (68 mg, 0.10 mmol) and **2** (28 mg, 0.11 mmol) in dry MeCN (7 mL) was stirred for 5 d. The reaction was worked up as described for **6**·4PF₆ to yield **33**·4PF₆ as an orange solid (46 mg, 28%). M.p.: >250 °C; ^1H NMR (400 MHz, CD_3CN , 313 K): $\delta = 8.86$ (d, 8H), 7.82 (s, 8H), 7.66 (d, 8H), 7.04 (d, $J = 8.5$ Hz, 2H), 6.74 (dd, $J = 1.8, 8.5$ Hz, 2H), 6.59 (d, $J = 2.0$ Hz, 2H), 5.73 (s, 8H), 4.10 (s, 4H), 3.54–4.12 (m, 36H); ^{13}C NMR (75 MHz, CD_3CN): $\delta = 158.1, 146.6, 145.3, 136.6, 131.7, 131.7, 130.3, 127.5, 127.1, 118.6, 117.0, 107.1, 72.9, 71.1, 71.1, 71.1, 70.9, 70.9, 70.9, 70.1, 68.4, 65.5$; MS (FAB): m/z (%) = 1714 (2) $[M^+]$, 1569 (16) $[M^+ - \text{PF}_6^-]$, 1424 (22) $[M^+ - 2\text{PF}_6^-]$, 1279 (6) $[M^+ - 3\text{PF}_6^-]$; $\text{C}_{70}\text{H}_{78}\text{F}_{24}\text{N}_4\text{O}_{10}\text{P}_4$ (1714): calcd C 49.01, H 4.58, N 3.27; found: C 48.83, H 4.47, N 3.17.

Absorption and luminescence measurements: Unless otherwise stated, room temperature experiments were carried out in air-equilibrated MeCN (spectrofluorimeter grade) solutions. Electronic absorption spectra were recorded with a Perkin–Elmer $\lambda 6$ spectrophotometer. Emission spectra and phosphorescence lifetimes were obtained with a Perkin–Elmer LS50 spectrofluorimeter. Emission spectra in a butyronitrile rigid matrix at 77 K were recorded with quartz tubes immersed in a quartz Dewar flask filled with liquid nitrogen. Fluorescence quantum yields were determined with either naphthalene in degassed cyclohexane ($\phi = 0.23$)^[28] or quinine sulfate in $\text{In H}_2\text{SO}_4$ ($\phi = 0.55$)^[29] as standards. Nanosecond and picosecond lifetime measurements were performed with an Edinburgh single-photon counter and a picosecond spectrometer based on a Nd YAG (PY62-10 Continuum) laser and a Hamamatsu C1587 streak camera.^[30] Experimental errors: absorption maxima, ± 2 nm; emission maxima, ± 2 nm; excited state lifetimes, $\pm 10\%$; and fluorescence quantum yields, $\pm 20\%$.

Acknowledgements: This research was supported by the Engineering and Physical Sciences Research Council (EPSRC) as well as by Merck Sharp & Dohme in the UK, and by the University of Bologna (Funds for Selected

Research Topics), MURST, and CNR (Progetto Strategico Tecnologie Chimiche Innovative) in Italy. We thank Dr. Lucia Flamigni (FRAE-CNR) for the picosecond measurements.

Received: June 30, 1997 [F741]

- [1] D. Philp, J. F. Stoddart, *Angew. Chem.* **1996**, *108*, 1242–1286; *Angew. Chem. Int. Ed. Engl.* **1996**, *35*, 1154–1196.
- [2] M. Gómez-López, J. A. Preece, J. F. Stoddart, *Nanotechnology* **1996**, *7*, 183–192.
- [3] For articles dealing with molecular recognition see: a) J. Rebek, Jr., *Angew. Chem.* **1990**, *102*, 261–272; *Angew. Chem. Int. Ed. Engl.* **1990**, *29*, 245–255; b) H.-J. Schneider, *Angew. Chem.* **1991**, *103*, 1419–1439; *Angew. Chem. Int. Ed. Engl.* **1991**, *30*, 1417–1436; c) F. Diederich, D. B. Smithrud, E. M. Sanford, T. B. Wyman, S. B. Ferguson, D. R. Carcanague, I. Chao, K. N. Houk, *Acta Chem. Scand.* **1992**, *46*, 205–215; d) M. Mascal, *Contemp. Org. Synth.* **1994**, *1*, 31–46; e) F. W. Lichtenhaler, *Angew. Chem.* **1994**, *106*, 2456–2467; *Angew. Chem. Int. Ed. Engl.* **1994**, *33*, 2364–2374.
- [4] J.-M. Lehn, *Supramolecular Chemistry—Concepts and Perspectives*, VCH, Weinheim, **1995**.
- [5] For examples of paraquat receptors, see: a) P. R. Ashton, E. J. T. Chrystal, J. P. Mathias, K. P. Parry, A. M. Z. Slawin, N. Spencer, J. F. Stoddart, D. J. Williams, *Tetrahedron Lett.* **1987**, *28*, 6367–6370; b) A. R. Bernado, T. Lu, E. Córdova, L. Zhang, G. W. Gokel, A. E. Kaifer, *J. Chem. Soc. Chem. Commun.* **1994**, 529–530; c) M. J. Gunter, M. R. Johnston, B. W. Skelton, A. H. White, *J. Chem. Soc. Perkin Trans. 1* **1994**, *116*, 1009–1018; d) A. P. H. Schenning, B. de Bruin, A. E. Rowan, H. Kooijman, A. L. Spek, R. J. M. Nolte, *Angew. Chem.* **1995**, *107*, 2288–2289; *Angew. Chem. Int. Ed. Engl.* **1995**, *34*, 2132–2134.
- [6] J. F. Stoddart, *Pure Appl. Chem.* **1988**, *60*, 467–472.
- [7] D. B. Amabilino, J. F. Stoddart, *Chem. Rev.* **1995**, *95*, 2725–2828.
- [8] P. R. Ashton, T. T. Goodnow, A. E. Kaifer, M. V. Reddington, A. M. Z. Slawin, N. Spencer, J. F. Stoddart, C. Vicent, D. J. Williams, *Angew. Chem.* **1989**, *101*, 1404–1408; *Angew. Chem. Int. Ed. Engl.* **1989**, *28*, 1396–1399.
- [9] a) M. H. Schwartz, *J. Incl. Phenom.* **1990**, *9*, 1–35; b) F. Cozzi, M. Cinquini, R. Annunziata, T. Dwyer, J. S. Siegel, *J. Am. Chem. Soc.* **1992**, *114*, 5729–5733; c) J. H. Williams, *Acc. Chem. Res.* **1993**, *26*, 593–598; d) C. A. Hunter, *Angew. Chem.* **1993**, *105*, 1653–1655; *Angew. Chem. Int. Ed. Engl.* **1993**, *32*, 1584–1586; e) F. Cozzi, M. Cinquini, R. Annunziata, J. S. Siegel, *J. Am. Chem. Soc.* **1993**, *115*, 5330–5331; f) C. A. Hunter, *J. Mol. Biol.* **1993**, *230*, 1025–1054; g) T. Dahl, *Acta Chem. Scand.* **1994**, *48*, 95–116; h) F. Cozzi, J. S. Siegel, *Pure Appl. Chem.* **1995**, *67*, 683–689.
- [10] a) M. C. Etter, *Acc. Chem. Res.* **1990**, *23*, 120–126; b) M. C. Etter, J. C. MacDonald, J. Bernstein, *Acta Crystallogr.* **1990**, *B46*, 256–262; c) A. D. Hamilton, *J. Chem. Ed.* **1990**, *67*, 821–828; d) G. R. Desiraju, *Acc. Chem. Res.* **1991**, *24*, 290–296; e) C. B. Aakeröy, K. R. Seddon, *Chem. Soc. Rev.* **1993**, *22*, 397–407; f) J. C. MacDonald, G. M. Whitesides, *Chem. Rev.* **1994**, *94*, 2383–2420; g) J.-M. Lehn, *Pure Appl. Chem.* **1994**, *66*, 1961–1966; h) J. Bernstein, R. E. Davis, L. Shimoni, N. L. Chang, *Angew. Chem.* **1995**, *107*, 1689–1708; *Angew. Chem. Int. Ed. Engl.* **1995**, *34*, 1555–1573; i) A. D. Burrows, C. W. Chan, M. L. Chowdhry, J. E. McGrady, D. M. P. Mingos, *Chem. Soc. Rev.* **1995**, *24*, 329–339; j) K. Endo, T. Sawaki, M. Koyanagi, K. Kobayashi, H. Masuda, Y. Aoyama, *J. Am. Chem. Soc.* **1995**, *117*, 8341–8352; k) M. L. Chowdhry, D. M. P. Mingos, A. J. P. White, D. J. Williams, *Chem. Commun.* **1996**, 899–900.
- [11] a) M. Nishio, M. Hirota, *Tetrahedron* **1989**, *45*, 7201–7245; b) M. Oki, *Acc. Chem. Res.* **1990**, *23*, 351–356; c) W. L. Jorgensen, D. L. Severance, *J. Am. Chem. Soc.* **1990**, *112*, 4768–4774; d) M. C. Etter, *J. Phys. Chem.* **1991**, *95*, 4601–4610; e) M. J. Zaworotko, *Chem. Soc. Rev.* **1994**, *23*, 283–288; f) M. Nishio, Y. Umezawa, M. Hirota, Y. Takeuchi, *Tetrahedron* **1995**, *51*, 8665–8701; g) C. A. Hunter, *Chem. Soc. Rev.* **1994**, *23*, 101–109; h) D. A. Dougherty, *Science* **1996**, *271*, 163–168.
- [12] Process I is defined as the circumrotation of the macrocyclic polyether through the cavity of the tetracationic cyclophane. Process II is

- defined as the circumrotation of the tetracationic cyclophane through the cavity of the macrocyclic polyether.
- [13] a) P. R. Ashton, R. Ballardini, V. Balzani, M. Blower, M. Ciano, M. T. Gandolfi, L. Pérez-García, L. Prodi, C. H. McLean, D. Philp, N. Spencer, J. F. Stoddart, M. S. Tolley, *New J. Chem.* **1993**, *17*, 689–695; b) D. B. Amabilino, P. R. Ashton, G. R. Brown, W. Hayes, J. F. Stoddart, M. S. Tolley, D. J. Williams, *J. Chem. Soc. Chem. Commun.* **1994**, 2479–2482; c) D. B. Amabilino, C. O. Dietrich-Buchecker, A. Livoreil, L. Pérez-García, J.-P. Sauvage, J. F. Stoddart, *J. Am. Chem. Soc.* **1996**, *118*, 3905–3913.
- [14] a) P. R. Ashton, R. Ballardini, V. Balzani, M. T. Gandolfi, D. J.-F. Marquis, L. Pérez-García, L. Prodi, J. F. Stoddart, M. Venturi, *J. Chem. Soc., Chem. Commun.* **1994**, 177–180; b) P. R. Ashton, L. Pérez-García, J. F. Stoddart, A. J. P. White, D. J. Williams, *Angew. Chem.* **1995**, *107*, 607–610; *Angew. Chem. Int. Ed. Engl.* **1995**, *34*, 571–574; c) P. R. Ashton, R. Ballardini, V. Balzani, A. Credi, M. T. Gandolfi, S. Menzer, L. Pérez-García, L. Prodi, J. F. Stoddart, M. Venturi, A. J. P. White, D. J. Williams, *J. Am. Chem. Soc.* **1995**, *117*, 11171–11197.
- [15] S. J. Langford, J. F. Stoddart, in *Magnetism: A Supramolecular Function* (Ed.: O. Kahn), Kluwer Academic, Dordrecht, **1996**, pp. 85–106.
- [16] V. Balzani, F. Scandola, *Supramolecular Photochemistry*, Horwood, Chichester (UK), **1991**.
- [17] a) R. A. Bissell, E. Córdova, A. E. Kaifer, J. F. Stoddart, *Nature (London)* **1994**, *369*, 133–137; b) M. J. Gunter, M. R. Johnston, *J. Chem. Soc. Chem. Commun.* **1994**, 829–830; c) M. Asakawa, S. Iqbal, J. F. Stoddart, N. D. Tinker, *Angew. Chem.* **1996**, *108*, 1054–1056; *Angew. Chem. Int. Ed. Engl.* **1996**, *35*, 976–978; d) M. Asakawa, S. Iqbal, J. F. Stoddart, N. D. Tinker, *Chem. Commun.* **1996**, 479–481; e) R. Ballardini, V. Balzani, A. Credi, M. T. Gandolfi, S. J. Langford, S. Menzer, L. Prodi, J. F. Stoddart, M. Venturi, D. J. Williams, *Angew. Chem.* **1996**, *108*, 1056–1059; *Angew. Chem. Int. Ed. Engl.* **1996**, *35*, 978–981; f) A. Credi, V. Balzani, S. J. Langford, J. F. Stoddart, *J. Am. Chem. Soc.* **1997**, *119*, 2679–2681. See also ref. [13c].
- [18] a) R. Ballardini, V. Balzani, M. T. Gandolfi, L. Prodi, D. Philp, H. G. Ricketts, J. F. Stoddart, M. Venturi, *Angew. Chem.* **1993**, *105*, 1362–1364; *Angew. Chem. Int. Ed. Engl.* **1993**, *32*, 1301–1303; b) M. Bauer, U. Müller, W. M. Müller, K. Rissanen, F. Vögtle, *Liebigs Ann.* **1995**, 649–656; c) A. C. Benniston, A. Harriman, V. M. Lynch, *J. Am. Chem. Soc.* **1995**, *117*, 5275–5291; d) P. R. Ashton, R. Ballardini, V. Balzani, S. E. Boyd, A. Credi, M. T. Gandolfi, M. Gómez-Lopéz, S. Iqbal, D. Philp, J. A. Preece, L. Prodi, H. G. Ricketts, J. F. Stoddart, M. S. Tolley, M. Venturi, A. J. P. White, D. J. Williams, *Chem. Eur. J.* **1997**, *3*, 152–170.
- [19] a) A. Livoreil, C. O. Dietrich-Buchecker, J.-P. Sauvage, *J. Am. Chem. Soc.* **1994**, *116*, 9399–9400; b) J.-P. Collin, P. Gaviña, J.-P. Sauvage, *Chem. Commun.* **1996**, 2005–2006; c) D. J. Cárdenas, A. Livoreil, J.-P. Sauvage, *J. Am. Chem. Soc.* **1996**, *118*, 11980–11981; d) C. Canevet, J. Libman, A. Shanzer, *Angew. Chem.* **1996**, *108*, 2842–2845; *Angew. Chem. Int. Ed. Engl.* **1996**, *35*, 2657–2659. See also refs. [14a,c].
- [20] P.-L. Anelli, P. R. Ashton, R. Ballardini, V. Balzani, M. Delgado, M. T. Gandolfi, T. T. Goodnow, A. E. Kalfner, D. Philp, M. Pietraszkiewicz, L. Prodi, M. V. Reddington, A. M. Z. Slawin, N. Spencer, J. F. Stoddart, C. Vicent, D. J. Williams, *J. Am. Chem. Soc.* **1992**, *114*, 193–218.
- [21] J. K. M. Sanders, B. K. Hunter, *Modern NMR Spectroscopy—A Guide for Chemists*, Oxford University Press, Oxford, **1992**.
- [22] a) I. O. Sutherland, *Ann. Rep. NMR Spectrosc.* **1971**, *4*, 71–235; b) J. Sandström, *Dynamic NMR Spectroscopy*, Academic Press, London, **1982**.
- [23] P. R. Ashton, R. Ballardini, V. Balzani, M. Belohradsky, M. T. Gandolfi, D. Philp, L. Prodi, F. M. Raymo, M. V. Reddington, A. M. Z. Slawin, N. Spencer, J. F. Stoddart, M. Venturi, D. J. Williams, *J. Am. Chem. Soc.* **1996**, *118*, 4931–4951.
- [24] R. Ballardini, V. Balzani, A. Credi, M. T. Gandolfi, F. Kotzyba-Hibert, J.-M. Lehn, L. Prodi, *J. Am. Chem. Soc.* **1994**, *116*, 5741–5746.
- [25] R. Ballardini, V. Balzani, M. Ciano, M. T. Gandolfi, F. Kohnke, L. Prodi, H. Shahriari-Zavareh, N. Spencer, J. F. Stoddart, *J. Am. Chem. Soc.* **1989**, *111*, 7072–7078.
- [26] M. T. Gandolfi, T. Zappi, R. Ballardini, L. Prodi, V. Balzani, J. F. Stoddart, J. P. Mathias, N. Spencer, *Gazz. Chim. Ital.* **1991**, *121*, 521–525.
- [27] W. L. Armarego, D. D. Perrin, *Purification of Laboratory Chemicals*, 3rd ed., Pergamon, New York, **1988**.
- [28] I. B. Berlman, *Handbook of Fluorescence Spectra of Aromatic Compounds*, Academic Press, London, **1971**.
- [29] W. H. Melhuish, *J. Phys. Chem.* **1961**, *65*, 229–235.
- [30] N. Armaroli, V. Balzani, F. Barigelletti, L. De Cola, L. Flamigni, J.-P. Sauvage, C. Hemmert, *J. Am. Chem. Soc.* **1994**, *116*, 5211–5217.